Dear Author

Here are the proofs of your article.

- You can submit your corrections **online,** via **e-mail** or by **fax**.
- For **online** submission please insert your corrections in the online correction form. Always indicate the line number to which the correction refers.
- You can also insert your corrections in the proof PDF and **email** the annotated PDF.
- For **fax** submission, please ensure that your corrections are clearly legible. Use a fine black pen and write the correction in the margin, not too close to the edge of the page.
- Remember to note the **journal title**, **article number**, and **your name** when sending your response via e-mail or fax.
- **Check** the metadata sheet to make sure that the header information, especially author names and the corresponding affiliations are correctly shown.
- **Check** the questions that may have arisen during copy editing and insert your answers/corrections.
- **Check** that the text is complete and that all figures, tables and their legends are included. Also check the accuracy of special characters, equations, and electronic supplementary material if applicable. If necessary refer to the *Edited manuscript*.
- The publication of inaccurate data such as dosages and units can have serious consequences. Please take particular care that all such details are correct.
- Please **do not** make changes that involve only matters of style. We have generally introduced forms that follow the journal's style.
- Substantial changes in content, e.g., new results, corrected values, title and authorship are not allowed without the approval of the responsible editor. In such a case, please contact the Editorial Office and return his/her consent together with the proof.
- If we do not receive your corrections **within 48 hours**, we will send you a reminder.
- Your article will be published **Online First** approximately one week after receipt of your corrected proofs. This is the **official first publication** citable with the DOI. **Further changes are, therefore, not possible.**
- The **printed version** will follow in a forthcoming issue.

Please note

After online publication, subscribers (personal/institutional) to this journal will have access to the complete article via the DOI using the URL:

`http://dx.doi.org/10.1007/s00441-015-2251-3`

If you would like to know when your article has been published online, take advantage of our free alert service. For registration and further information, go to: http://www.link.springer.com.

Due to the electronic nature of the procedure, the manuscript and the original figures will only be returned to you on special request. When you return your corrections, please inform us, if you would like to have these documents returned.

Metadata of the article that will be visualized in OnlineFirst

1	Article Title	**Alterations in the distal colon innervation in *Winnie* mouse model of spontaneous chronic colitis**	
2	Article Sub- Title		
3	Article Copyright - Year	**Springer-Verlag Berlin Heidelberg 2015 (This will be the copyright line in the final PDF)**	
4	Journal Name	Cell and Tissue Research	
5	Corresponding Author	Family Name	**Nurgali**
6		Particle	
7		Given Name	**Kulmira**
8		Suffix	
9		Organization	Victoria University
10		Division	Centre for Chronic Disease, College of Health and Biomedicine
11		Address	Melbourne, Australia
12		Organization	Western Centre for Health, Research and Education
13		Division	
14		Address	176 Furlong Road, St Albans 3021, Victoria, Australia
15		e-mail	Kulmira.Nurgali@vu.edu.au
16	Author	Family Name	**Rahman**
17		Particle	
18		Given Name	**Ahmed A.**
19		Suffix	
20		Organization	Victoria University
21		Division	Centre for Chronic Disease, College of Health and Biomedicine
22		Address	Melbourne, Australia
23		e-mail	
24	Author	Family Name	**Robinson**
25		Particle	
26		Given Name	**Ainsley M.**
27		Suffix	

28		Organization	Victoria University
29		Division	Centre for Chronic Disease, College of Health and Biomedicine
30		Address	Melbourne, Australia
31		e-mail	
32	Author	Family Name	**Jovanovska**
33		Particle	
34		Given Name	**Valentina**
35		Suffix	
36		Organization	Victoria University
37		Division	Centre for Chronic Disease, College of Health and Biomedicine
38		Address	Melbourne, Australia
39		e-mail	
40	Author	Family Name	**Eri**
41		Particle	
42		Given Name	**Rajaraman**
43		Suffix	
44		Organization	The University of Tasmania
45		Division	School of Health Sciences
46		Address	Launceston, Australia
47		e-mail	

48	Schedule	Received	15 March 2015
49		Revised	
50		Accepted	29 June 2015

51 Abstract

The gastrointestinal tract is innervated by extrinsic sympathetic, parasympathetic and sensory nerve fibers as well as by intrinsic fibers from the neurons in myenteric and submucosal ganglia embedded into the gastrointestinal wall. Morphological and functional studies of intestinal innervation in animal models are important to understand the pathophysiology of inflammatory bowel disease (IBD). The recently established *Winnie* mouse model of spontaneous chronic colitis caused by a point mutation in the *Muc2* mucin gene develops inflammation due to a primary epithelial defect. *Winnie* mice display symptoms of diarrhea, ulcerations and rectal bleeding similar to those in IBD. In this study, we investigated myenteric neurons, noradrenergic, cholinergic and sensory nerve fibers in the distal colon of *Winnie* (*Win/Win*) mice compared to C57/BL6 and heterozygote littermates (*Win/Wt*) using histological and immunohistochemical methods. All *Win/Win* mice used in this study had inflammation with signs of mucosal damage, goblet cell loss, thickening of muscle and mucosal layers, and increased

		CD45-immunoreactivity in the distal colon. The density of sensory, cholinergic and noradrenergic fibers innervating the myenteric plexus, muscle and mucosa significantly decreased in the distal colon of *Win/Win* mice compared to C57/BL6 and *Win/Wt* mice, while the total number of myenteric neurons as well as subpopulations of cholinergic and nitrergic neurons remained unchanged. In conclusion, changes in the colon morphology and innervation found in *Winnie* mice have multiple similarities with changes observed in patients with ulcerative colitis.
52	Keywords separated by ' - '	Myenteric neurons - Spontaneous chronic colitis - *Winnie* mice - Distal colon - Innervation
53	Foot note information	

Cell Tissue Res
DOI 10.1007/s00441-015-2251-3

REGULAR ARTICLE

Alterations in the distal colon innervation in *Winnie* mouse model of spontaneous chronic colitis

Ahmed A. Rahman[1] · **Ainsley M. Robinson**[1] · **Valentina Jovanovska**[1] · **Rajaraman Eri**[2] · **Kulmira Nurgali**[1,3]

Received: 15 March 2015 / Accepted: 29 June 2015

Abstract The gastrointestinal tract is innervated by extrinsic sympathetic, parasympathetic and sensory nerve fibers as well as by intrinsic fibers from the neurons in myenteric and submucosal ganglia embedded into the gastrointestinal wall. Morphological and functional studies of intestinal innervation in animal models are important to understand the pathophysiology of inflammatory bowel disease (IBD). The recently established *Winnie* mouse model of spontaneous chronic colitis caused by a point mutation in the *Muc2* mucin gene develops inflammation due to a primary epithelial defect. *Winnie* mice display symptoms of diarrhea, ulcerations and rectal bleeding similar to those in IBD. In this study, we investigated myenteric neurons, noradrenergic, cholinergic and sensory nerve fibers in the distal colon of *Winnie* (*Win/Win*) mice compared to C57/BL6 and heterozygote littermates (*Win/Wt*) using histological and immunohistochemical methods. All *Win/Win* mice used in this study had inflammation with signs of mucosal damage, goblet cell loss, thickening of muscle and mucosal layers, and increased CD45-immunoreactivity in the distal colon. The density of sensory, cholinergic and noradrenergic fibers innervating the myenteric plexus, muscle and mucosa significantly decreased in the distal colon of *Win/Win* mice compared to C57/BL6 and *Win/Wt* mice, while the total number of myenteric neurons as well as subpopulations of cholinergic and nitrergic neurons remained unchanged. In conclusion, changes in the colon morphology and innervation found in *Winnie* mice have multiple similarities with changes observed in patients with ulcerative colitis.

Keywords Myenteric neurons · Spontaneous chronic colitis · *Winnie* mice · Distal colon · Innervation

Introduction

Inflammatory bowel disease (IBD) is a chronic inflammatory condition characterized by frequent relapses of disease activity and periods of remission that affect individuals throughout life (Podolsky 2002). The etiology of IBD is not completely understood. However, it is generally agreed that altered immunological function, resulting from a complex interplay between genetic susceptibility and certain environmental factors, contributes significantly to the initiation and progression of gastrointestinal (GI) inflammation (Kaser et al. 2010). IBD is comprised of two main immunologically and histopathologically different diseases, ulcerative colitis and Crohn's disease. A non-conventional TH2 immune response associated with epithelial barrier dysfunction has been implicated in the pathogenesis of ulcerative colitis, while elevated level of cytokines such as interferon-γ, interleukin-2, and tumor necrosis factor-α in the gut consistent with a TH1 type response plays an important role in the pathogenesis of Crohn's disease (Strober et al. 2007). Ulcerative colitis causes inflammation and ulcers in the mucosal lining of the large intestine whereas all layers of the gut wall may be affected in Crohn's disease. Inflammation in the gut causes breakdown of intestinal barrier function and abnormal secretion, changes in muscle contractility, neurotransmission, visceral sensation and motility patterns leading to symptoms of diarrhea, cramping and pain (Belai et al. 1997; Jönsson

✉ Kulmira Nurgali
Kulmira.Nurgali@vu.edu.au

[1] Centre for Chronic Disease, College of Health and Biomedicine, Victoria University, Melbourne, Australia

[2] School of Health Sciences, The University of Tasmania, Launceston, Australia

[3] Western Centre for Health, Research and Education, 176 Furlong Road, St Albans 3021, Victoria, Australia

et al. 2007; Mayer and Gebhart 1994; Neunlist et al. 2003; Rao and Read 1990; Straub et al. 2008).

Several lines of evidence indicating abnormal structural and functional alterations in the intrinsic and extrinsic innervation of the GI tract associate with symptoms of IBD (Bernardini et al. 2012; Geboes and Collins 1998; Lindgren et al. 1991, 1993; Moynes et al. 2014). The enteric nervous system (ENS), residing within the gut wall and innervating mucosa, muscles and glands, controls GI functions such as nutrient absorption, secretion, GI sensation and propulsion of the contents along the gut (intestinal motility) (Furness 2012). Intestinal inflammation induces morphological and functional changes in the ENS (Mawe et al. 2009). Functional changes involve shifts in the amount and proportion of neurotransmitters and neuropeptides in the ENS of IBD patients and animal models of intestinal inflammation (Boyer et al. 2005; Neunlist et al. 2003; Winston et al. 2013). Alterations in electrophysiological properties of enteric neurons and in neurotransmission between enteric neurons and to the intestinal muscles have been found in animal models of intestinal inflammation (Linden et al. 2003; Lomax et al. 2005; Nurgali et al. 2007, 2009, 2011). These changes in the ENS correlate with intestinal dysmotility (Krauter et al. 2007; Lomax et al. 2007a; Winston et al. 2013). Alterations in the structure and function of cholinergic and noradrenergic nerve fibers innervating the gut wall and synapsing on the enteric neurons have been observed in patients with IBD (Straub et al. 2008), as well as in animal models of intestinal inflammation (Lomax et al. 2010; Swain et al. 1991). Studies of inflammation-induced damage to the ENS and extrinsic nerve fibers in the inflamed intestine are of great significance for understanding mechanisms underlying intestinal dysfunctions and identification of new targets for effective therapies.

More than 60 experimental animal models have been established to study IBD, including genetically engineered mice, chemically-induced models, congenic mouse strains, and immune cell transfer models (Mizoguchi 2012). Although these models do not reproduce the complexity of human disease, they are valuable tools for studying many important aspects of the pathophysiological mechanisms and the effects of emerging therapeutic strategies (Wirtz and Neurath 2007). Most of the experimental models induce acute colitis, while there are only a few animal models of chronic intestinal inflammation. Recently, the *Winnie* mouse model of colitis has been developed. In this model, chronic intestinal inflammation results from a primary intestinal epithelial defect conferred by a point mutation rather than a deletion in the *Muc2* mucin gene (Eri et al. 2011; Heazlewood et al. 2008). In humans, expression of *Muc2* is reduced or depleted in Crohn's disease (Buisine et al. 2001), while in active ulcerative colitis, *Muc2* production and secretion are reduced (Van Klinken et al. 1999). *Winnie* mice (C57/BL6 background) show abnormal *Muc2* biosynthesis causing changes in a mucus layer, increased intestinal permeability and greatly enhanced susceptibility to luminal inflammation-inducing toxins. They develop mild spontaneous inflammation in the distal colon with symptoms comparable to human IBD by 6 weeks of age; inflammation progresses over time and results in severe colitis by the age of 16 weeks (Eri et al. 2011; McGuckin et al. 2011). Colitis in *Winnie* mice is chronic with periods of remissions and relapses similar to human IBD. Previous studies consist mainly of histopathological and immunological changes in the GI tract of *Winnie* mice, but a study of the intestinal innervations in this model has not been performed. Since *Winnie* mice closely mimic human chronic colitis, the aim of the present investigation was to evaluate the intrinsic and extrinsic intestinal innervation, especially in the distal colon.

Materials and methods

Animals

Winnie (*Win/Win*) (19–26 g, 12–16 w.o., $n=16$), heterozygote littermates (*Win/Wt*) (20–25 g, $n=16$) and age-matched C57/BL6 (26–30 g, $n=16$) mice were obtained from Monash Animal Services (Melbourne, Australia). All mice were housed in a temperature-controlled environment with 12 h day/night cycles at the animal holding room at the Western Center for Health, Research and Education (Melbourne, Australia). All animal experiments in this study complied with the guidelines of the Australian Code of Practice for the Care and Use of Animals for Scientific Purposes and were approved by the Victoria University Animal Experimentation Ethics Committee. Mice were killed by cervical dislocation. Subsequent procedures were carried out in vitro.

Immunohistochemistry and histology

Immunohistochemistry was performed as described previously (Robinson et al. 2014; Wafai, et al. 2013). Briefly, segments of the distal colon were processed in two different ways: (1) wholemount longitudinal muscle-myenteric plexus (LMMP) preparations, and (2) cross-sections of the distal colon. In general, the colon was exposed through a midline laparotomy and a 5-cm section 2 cm from the anus was collected from each animal. Immediately following dissection, colon tissues were placed in oxygenated phosphate-buffered saline (PBS, pH 7.2) containing L-type Ca^{2+} channel blocker, nicardipine (3 μM). Segments of the distal colon were then cut open along the mesenteric border and pinned flat with the mucosal side up in a Sylgard-lined Petri dish (maximally stretched for LMMP preparations while unstretched for cross-sections). Tissues for LMMP preparations and cryostat cross-sections were fixed with Zamboni's fixative (2 % formaldehyde containing 0.2 % picric acid) overnight at 4 °C and subsequently washed

with dimethyl sulfoxide (DMSO) (Sigma-Aldrich, Australia) (3×10 min) followed by PBS (3×10 min). Tissues for histology were fixed in 10 % buffered formalin overnight at 4 °C and stored in 70 % ethanol until embedding.

For LMMP preparations, tissues were dissected to expose the myenteric plexus by removing the mucosa, submucosa and circular muscle layers. Following a 1 h incubation in 10 % normal donkey serum (Merck Millipore, MA, USA) at room temperature, tissues were incubated with primary antibodies against protein gene product (PGP) 9.5 (chicken, 1:500; Abcam, Cambridge, UK), CD45 (rat, 1:500; Biolegend, USA), neuronal nitric oxide synthase (nNOS) (goat, 1:500; Novus Biologicals, USA), choline acetyl transferase (ChAT, Goat, 1:500; Merck Millipore, Australia), vesicular acetylcholine transporter (VAChT) (goat, 1:500; Merck Millipore, Australia) and tyrosine hydroxylase (TH) (sheep, 1:1000; Merck Millipore, Australia). Anti-PGP9.5 antibody is a widely used marker for labeling all neuronal cell bodies (Kajimoto et al. 1992); anti-CD45 antibody is a pan leukocyte marker; anti-nNOS antibody identifies predominantly inhibitory muscle motor neurons and some interneurons (Qu et al. 2008); anti-ChAT antibody labels excitatory muscle motor neurons and interneurons; anti-VAChT antibody identifies cholinergic fibers (Qu et al. 2008; Weihe et al. 1996); and anti-TH antibody identifies noradrenergic fibers (Nagatsu 1989). The tissues were then washed briefly in PBS-Triton (0.1 %) and incubated with secondary antibodies: Alexa Fluor 594 (donkey anti-chicken, 1:200), Alexa Fluor 488 (donkey anti-goat, 1:200, donkey anti-sheep, 1:200) (Jackson ImmunoResearch, PA, USA) and mounted onto glass slides with fluorescent mounting medium (DAKO, Australia).

For cryostat cross-section preparations, tissues were cryoprotected (30 % sucrose/phosphate buffer; Sigma-Aldrich, Australia) overnight at 4 °C then transferred to 50 % Optimal Cutting Temperature compound (OCT; Tissue-Tek; Sakura Finetek, Torrance, CA, USA) in 30 % sucrose/phosphate buffer solution for 12 hr prior to freezing in 100 % OCT. Tissues were sectioned at a 20-μm thickness (at least 15 sections from each animal) using a cryostat microtome (Leica CM1850, St. Gallen, Switzerland) and mounted onto glass slides. Cross-sections were incubated with species-specific primary antibodies to detect CD45 (rat, 1:500; Biolegend), calcitonin gene-related peptide (CGRP) (rabbit, 1:3000; Sigma-Aldrich, MO, USA), TH (sheep, 1:1000; Merck Millipore, Australia) and VAChT (goat, 1:500; Merck Millipore, Australia). Intrinsic primary afferent neurons contain and release CGRP (Grider 2003). Additionally, approximately 85 % of spinal afferents and less than 5 % of vagal afferents contain CGRP, thus anti-CGRP antibody is recognized as a marker for sensory afferent fibers (Kressel et al. 1994). Sections were then washed in PBS and incubated with fluorophore-conjugated secondary antibodies Alexa Fluor 594 (donkey anti-rabbit, 1:200; Abacus ALS, Australia), Alexa Fluor 488 (donkey anti-rat, donkey anti-goat, 1:200; Jackson ImmunoResearch, PA, USA) and FITC (donkey anti-sheep, 1:200; Abacus ALS).

For histology, tissues were embedded in paraffin, sectioned at 5 μm, deparaffinized, cleared, and rehydrated in graded ethanol concentrations. For hematoxylin and eosin (H&E) staining, sections were immersed in Xylene (3×4 mins, 100 % ethanol (3 min), 90 % ethanol, (2 min), 70 % ethanol (2 min), rinsed in tap water, hematoxylin (4 min), rinsed in tap water, Scott's tap water (1 min), eosin (6 min), rinsed in tap water, 100 % ethanol (2×1 min), xylene (2×3 mins)and mounted on glass slides with DPX mountant.

Imaging

Images were captured using a Nikon Eclipse Ti multichannel confocal laser scanning system (Nikon, Japan). Immunolabeled sections were visualized and imaged by using filter combinations appropriate for the specific fluorophores such as FITC, Alexa 488 or 594 (488 or 559 nm excitation). Images (512×512 pixels) were obtained with 2×0 (dry, 0.75) or 40x (oil immersion, 1.3) lenses. In order to obtain Z-series, neuronal structures were imaged by collecting ten consecutive optical sections at 1-μm intervals. H&E stained colon sections were visualized using an Olympus microscope (Olympus BX53) and images were captured with CellSense™ software.

Quantitative analysis of immunohistochemical and histological data

Images were analyzed using Image J software (National Institute of Health, Bethesda, MD, USA). Muscle and mucosal thicknesses were quantified as described previously (Miampamba and Sharkey 1998). Muscle thickness was measured from the serosa to the submucosa including both longitudinal and circular muscle layers, while mucosal thickness was measured from the submucosa to the luminal surface of mucosa. Infiltration of leukocytes within the colon mucosa was assessed by measuring the density of CD45-immunoreactive (IR) cells per area (average of 8 areas of 500 μm^2 per animal at ×20 magnification). Image J software was employed to adjust color images from RGB to 8 bit, after which thresholding to a consistent value was applied to obtain the percentage area of CD45-immunoreactivity. Histological scores were developed from the following parameters: aberrant crypt architecture (score range 0–3), increased crypt length (0–3), goblet cell depletion (0–3), crypt abscesses (0–3), leukocyte infiltration (0–3), epithelial damage and ulceration (0–3) (average of 8 areas of 500 μm^2 per animal). Nerve fibers in cross-sections of the distal colon were measured from

8 images per preparation at ×20 magnification (total area 2 mm^2). Images were changed from RGB to 8 bit and made binary prior to particle analysis with Image J software. Myenteric neurons and CD45-IR leukocytes were counted in wholemount preparations within a 2-mm^2 area by randomly capturing 8 images per preparation at ×20 magnification. The number of neurons per ganglion was quantified in images at ×40 magnification; the number of neurons was averaged per 10 ganglia in each preparation.

Analysis of fecal water content and colon length

Fecal water content was calculated following stool collection from animals in all groups. After collection, stools were immediately weighed (wet weight) and left to air dry. Three days later, stools were re-weighed (dry weight) and the difference between wet and dry weight was calculated. Mouse colon length (from cecum to anus) was measured immediately after dissection from the animal by placing the colon parallel to a ruler and recording its size.

Statistical analysis

Statistical analysis was conducted with Prism (v.5.0; GraphPad Software, La Jolla, CA, USA). All values are expressed as mean ± standard error of the mean. Paired *t* tests were used to analyze the difference in weight, muscle and mucosal thickness. One-way ANOVA for multiple group comparison followed by the Bonferroni's or Tukey–Kramer post hoc tests was used to analyze the differences between all groups. $P<0.05$ was considered significant.

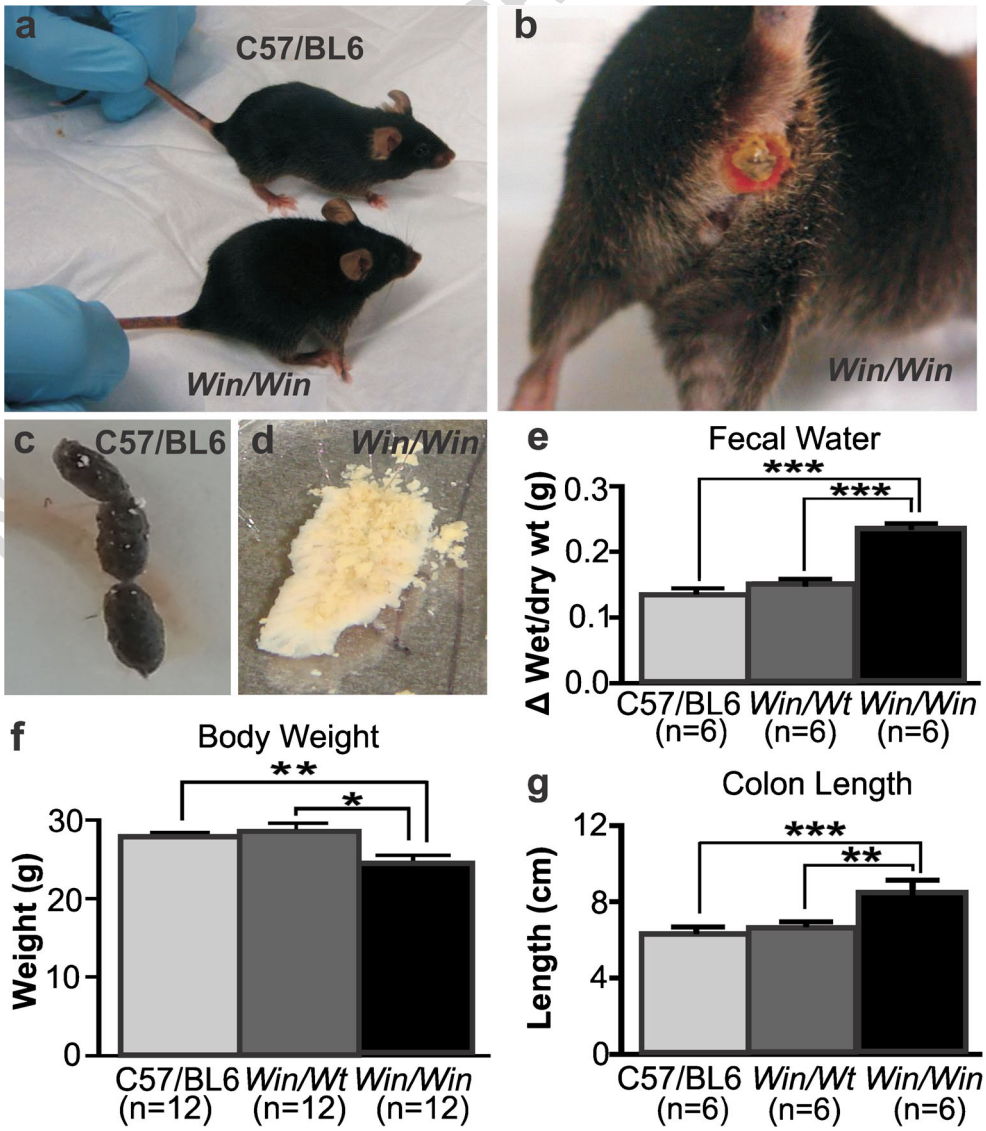

Fig. 1 *Winnie* mouse model of spontaneous chronic colitis. **a**, **b** Representative images of C57/BL6 (control) and *Winnie* (*Win/Win*) mice. *Win/Win* mice have hunchbacked posture, perianal inflammation, bleeding and soiled fur due to chronic diarrhea. **c**, **d** Soft fecal masses not forming pellets confirm non-watery diarrhea in *Win/Win* mice (**d**) compared to regular pellets in healthy C57/BL6 mice (**c**). **e** Fecal water content calculated as the difference (Δ) between wet and dry stool weight (wt) was higher in *Win/Win* mice. **f** *Win/Win* mice have lower average body weight compared to C57/BL6 mice and heterozygote littermates (*Win/Wt*). **g** Variation in colon length between C57/BL6, *Win/Wt* and *Win/Win* mice. Data are expressed as mean ± SEM. Numbers of animals are shown in *parentheses*. **P*<0.05, ***P*<0.01, ***P*<0.001

Results

Winnie mouse model of colitis

All *Win/Win* mice used in this study displayed symptoms of intestinal inflammation: perianal inflammation and bleeding, soiled fur and soft fecal consistency, not forming pellets compared to control mice (Fig. 1a–d). The fecal water content (wet weight minus dry weight) of stools from *Win/Win* mice was greater than in stools from C57/BL6 and *Win/Wt* mice ($P<0.001$ for both, $n=6$/per group; Fig. 1e; Table 1). The body weight of all mice was monitored daily for a period of 7 days prior to culling. Average body weight of *Win/Win* mice (23±1.0 g) was less compared to C57/BL6 (27±0.2 g, $P<0.01$) and *Win/Wt* (28±0.3 g, $P<0.05$) mice ($n=12$/per group; Fig. 1f). Immediately following dissection, the length of the colon was measured and recorded showing *Win/Win* mice to have longer colons compared to C57/BL6 ($P<0.001$) and *Win/Wt* ($P<0.01$) mice ($n=6$/per group; Fig. 1g; Table 1).

Consistent with observations from previously published studies (Eri et al. 2011; Heazlewood et al. 2008; McGuckin et al. 2011), *Win/Win* mice demonstrated prominent mucosal damage with epithelial exfoliation, leukocyte infiltration, crypt elongation and abscesses, goblet cell loss and destruction of the mucosal architecture (Fig. 2a–c). No abnormalities were observed in the histology of the colon from C57/BL6 mice while only very mild inflammatory changes were observed in *Win/Wt* mice (Fig. 2a–c).

Thickening of the muscle layer is also considered as a histological index of inflammation (Miampamba and Sharkey 1998). The thickness of the colonic muscle layer (total thickness of longitudinal and circular muscles) was significantly higher in *Win/Win* mice (50±1.4 μm, $n=4$) compared to both C57/BL6 (44±0.6 μm, $P<0.05$, $n=4$) and *Win/Wt* mice (45±1.2 μm, $P<0.01$, $n=4$; Fig. 2d). *Win/Win* mice had a significantly thicker mucosal layer (271±5 μm, $n=4$) compared to C57/BL6 (206±4 μm, $P<0.001$, $n=4$) and *Win/Wt* mice (197±6 μm, $P<0.01$, $n=4$; Fig. 2e).

The severity of inflammation was evaluated by immunolabelling with anti-CD45 antibody specific to the leukocyte common antigen in cross-sections of the colon (Fig. 2f-h). Quantification of leukocyte density in the distal colon revealed a higher level of leukocyte infiltration within the mucosa of *Win/Win* mice compared to C57/BL6 and *Win/Wt* mice ($P<0.01$ for both, $n=6$/per group; Fig. 2i; Table 1). Infiltration of CD45-IR cells to the level of myenteric ganglia was studied in wholemount LMMP preparations. Quantitative analysis did not reveal significant difference between the groups (data not shown). In cross-sections, gross morphological damage was assessed to further substantiate the level of inflammation in the distal colon of mice from all groups. Histological scoring of H&E-stained sections incorporated individual scores for various parameters: aberrant crypt architecture, increased crypt length, goblet cell depletion, general leukocyte infiltration, crypt abscesses and epithelial damage and ulceration.

Assessment of all parameters revealed histological scores to be significantly higher in sections from *Win/Win* mice compared to sections from C57/BL6 and *Win/Wt* mice ($P<0.001$ for all, $n=6$/per group; Fig. 2j; Table 1).

Table 1 Evaluation of intestinal inflammation

Parameter		C57/BL6	*Win/Wt*	*Win/Win*
Diarrhea ($n=12$/group)		Absent (hard pellets)	Absent (hard pellets)	Prominent (loose stool)
Fecal water content (wet weight minus dry weight, g) ($n=6$/group)		0.14±0.005	0.15±0.004	0.24±0.005***
Colon length (from caecum to anus, cm) ($n=6$/group)		6.2±0.2	6.4±0.2	8.3±0.5$^{###, ††}$
Density of CD45+ leukocytes in colon cross-sections (average within 2 mm^2 per animal, %) ($n=6$/group)		6.6±0.5	8.0±0.9	12.9±1.5***
Parameters for histological scoring ($n=4$/group)	Aberrant crypt architecture (0–3)	0.33±0.05	0.42±0.21	2.33±0.06***
	Increased crypt length (0–3)	0.25±0.04	0.33±0.02	2.33±0.05***
	Goblet cell depletion (0–3)	0.25±0.03	0.33±0.08	2.25±0.03***
	General leukocyte infiltration (0–3)	0.17±0.1	0.33±0.1	2.25±0.12***
	Crypt abscesses (0–3)	0.25±0.15	0.25±0.15	2.50±0.15***
	Epithelial damage and ulceration (0–3)	0.33±0.34	0.42±0.14	2.55±0.35***
Overall histological score (out of 18) ($n=4$/group)		3.1±0.6	4.4±0.4	14.4±0.6***

***$P<0.001$ compared to both C57/BL6 and *Win/Wt* groups

$^{###}$ $P<0.001$ compared to C57/BL6 group

†† $P<0.01$ compared to *Win/Wt* group

JnlID 441_ArtID 2251_Proof# 1 - 09/07/2015

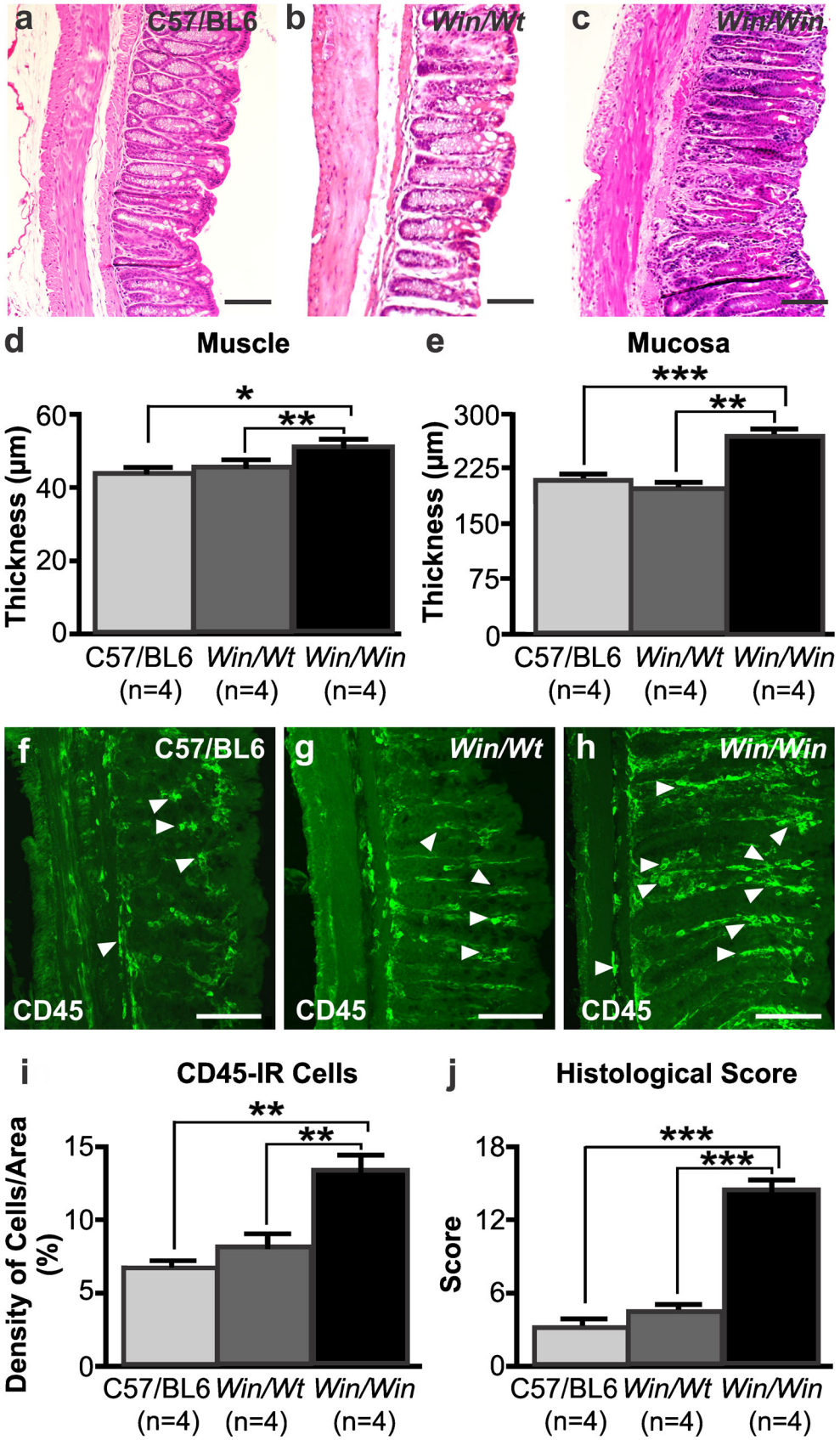

◀ **Fig. 2** Histological and immunohistochemical evidence of colitis in *Winnie* mice. **a**–**c** Hematoxylin and eosin staining of the distal colon sections from C57/BL6, heterozygote (*Win/Wt*) and *Winnie* (*Win/Win*) mice. *Scale bars* 100 μm. **d**, **e** Increased thickness of muscle layers and elongation of crypts observed in the distal colon from *Win/Win* compared to C57/BL6 and *Win/Wt* mice. **f**–**h** Anti-CD45 antibody labelling of leukocyte infiltration (*arrowheads*) within the colon wall. *Scale bars* 100 μm. **i** Density of CD45-IR cells per 0.5 mm^2 in colon sections from C57/BL6, *Win/Wt* and *Win/Win* mice. **j** Overall histological score based on the analysis of six individual parameters from H&E-stained sections. Data are expressed as mean ± SEM. Numbers of animals are shown in *parentheses*. **P*<0.05, ***P*<0.01. ****P*<0.001

Changes in the density of cholinergic nerve fibers in the distal colon of *Winnie* mice

Anti-VAChT antibody was used as a marker for cholinergic fibers accumulating acetylcholine in synaptic vesicles (Qu et al. 2008; Weihe et al. 1996) in both cross-sections and wholemount LMMP preparations of the distal colon. The density of cholinergic fibers was decreased within both mucosal and muscle layers observed in the cross-section preparations from *Win/Win* (4.7±0.2 %, *n*=4) compared to C57/BL6 (6.4±0.3 %, *P*<0.05, *n*=4) and *Win/Wt* (6.1±0.4 %, *P*<0.05, *n*=4) mice (Fig. 3a–c, g). Similarly, a significant decrease in VAChT-IR fibers within the myenteric ganglia was observed in wholemount LMMP preparations of the distal colon from *Win/Win* (5.2±0.4 %, *n*=4) compared to C57/BL6 (8.6±0.6 %, *P*<0.01, *n*=4) and *Win/Wt* (7.7±0.7 %, *P*<0.05, *n*=4) mice (Fig. 3d–f, h).

Changes in the density of noradrenergic and sensory nerve fibers in the distal colon of *Winnie* mice

TH immunoreactivity was used to label sympathetic fibers in the gastrointestinal tract (Lourenssen et al. 2005; Straub et al.

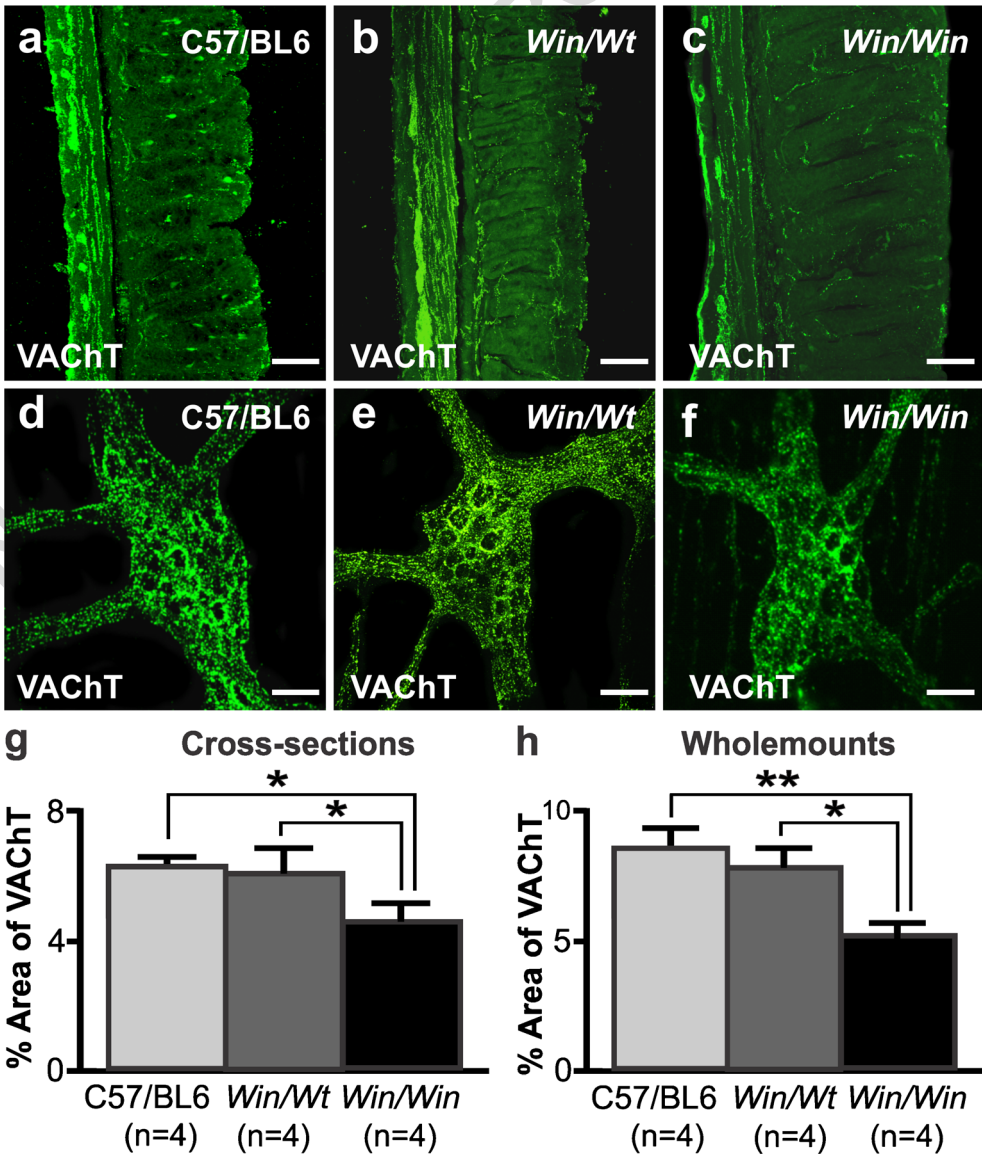

Fig. 3 Cholinergic nerve fiber density in the mucosa and myenteric ganglia in the distal colon of *Winnie* mice. Antibody against vesicular acetylcholine transporter (*VAChT*) was used to label cholinergic fibers in cross-sections (**a**–**c**) and wholemount preparations of the myenteric ganglia (**d**–**f**). *Scale bars* 100 μm. Significant decrease in the VAChT-IR fiber density observed in cross-sections (**g**) as well as in wholemount preparations (**h**) of the distal colon from *Winnie* (*Win/Win*) mice compared to C57/BL6 and heterozygote littermates (*Win/Wt*). Data are expressed as mean ± SEM. Numbers of animals are shown in *parentheses*. **P*<0.05, ***P*<0.01

JmlID 441_ArtID 2251_Proof# 1 - 09/07/2015

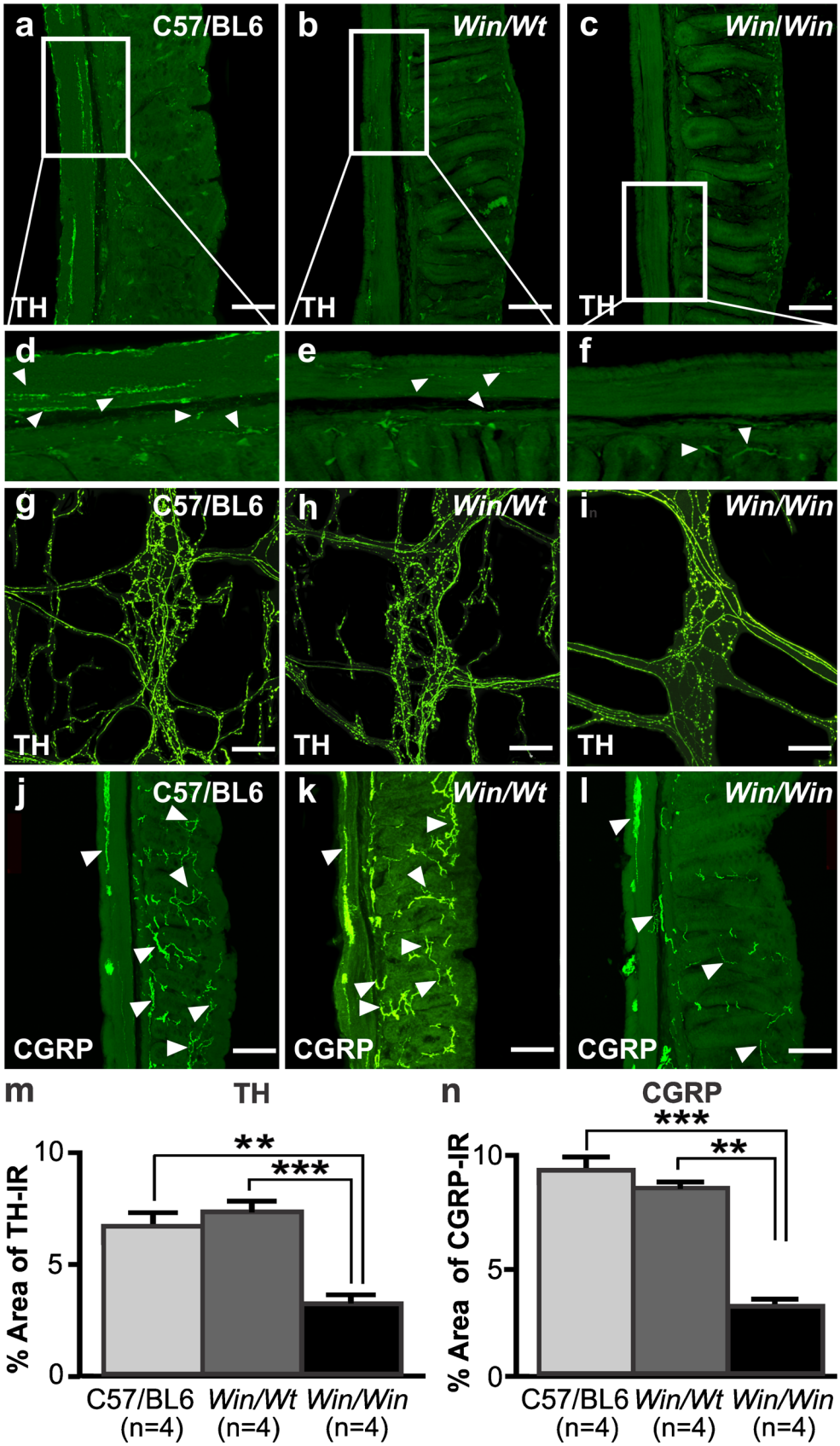

◀ **Fig. 4** Density of noradrenergic and sensory nerve fibers in the distal colon of *Winnie* mice. Noradrenergic fibers labeled using anti-tyrosine hydroxylase (*TH*) antibody were observed in cross-sections (**a**–**f**) and in wholemount preparations of the distal colon myenteric ganglia (**g**–**i**). **j**–**l** Sensory fibers labeled using antibody against calcitonin gene-related peptide (*CGRP*) were observed in the cross-sections of the distal colon. *Scale bars* 100 μm. Quantitative analysis revealed significant reduction in the density of TH-IR fibers in wholemount preparations (**m**) and CGRP-IR fibers in cross-sections (**n**) of the distal colon from *Win/Win* compared to C57/BL6 and *Win/Wt* mice. Data are expressed as mean ± SEM. Numbers of animals are shown in *parentheses*. $^{**}P<0.01$; $^{***}P<0.001$

2008; Chen et al. 2015) as well as cell bodies of intrinsic noradrenergic and dopaminergic neurons (Li et al. 2004; Qu et al. 2008). In our study, TH-IR neurons were not found in the distal colon of C57/BL6, *Win/Win* or *Win/Wt* mice. To assess changes in the expression of noradrenergic fibers, we evaluated the density of TH-IR fibers in both cross-sections and wholemount LMMP preparations of the distal colon in *Win/Win* mice compared to C57/BL6 and *Win/Wt* mice (Fig. 4a–i). We were not able to quantify the fiber density in cross-sections due to very sparse amount of TH-IR fibers (Fig. 4a–f). However, quantitative analysis of TH-IR fibers was performed in wholemount preparations. A significant decrease in the density of TH-IR fibers within myenteric ganglia was observed in wholemount preparations of the distal colon from *Win/Win* (3.2±0.2 %, $n=4$) compared to C57/BL6 (6.6±0.7 %, $P<0.01$, $n=4$) and *Win/Wt* (7.3±0.5 %, $P<0.001$, $n=4$) mice (Fig. 4g–i, m).

Immunolabeling using anti-CGRP antibody was carried out to reveal sensory nerve fibers in the colon cross-sections. CGRP-IR nerve fibers were widely distributed in the mucosa, submucosal and myenteric plexuses of the colon in C57/BL6 and *Win/Wt* mice (Fig. 4j–l). A significant decrease in the density of CGRP-IR nerve fibers was observed in the colon cross-section preparations from *Win/Win* (3.3±0.1 %, $n=4$)

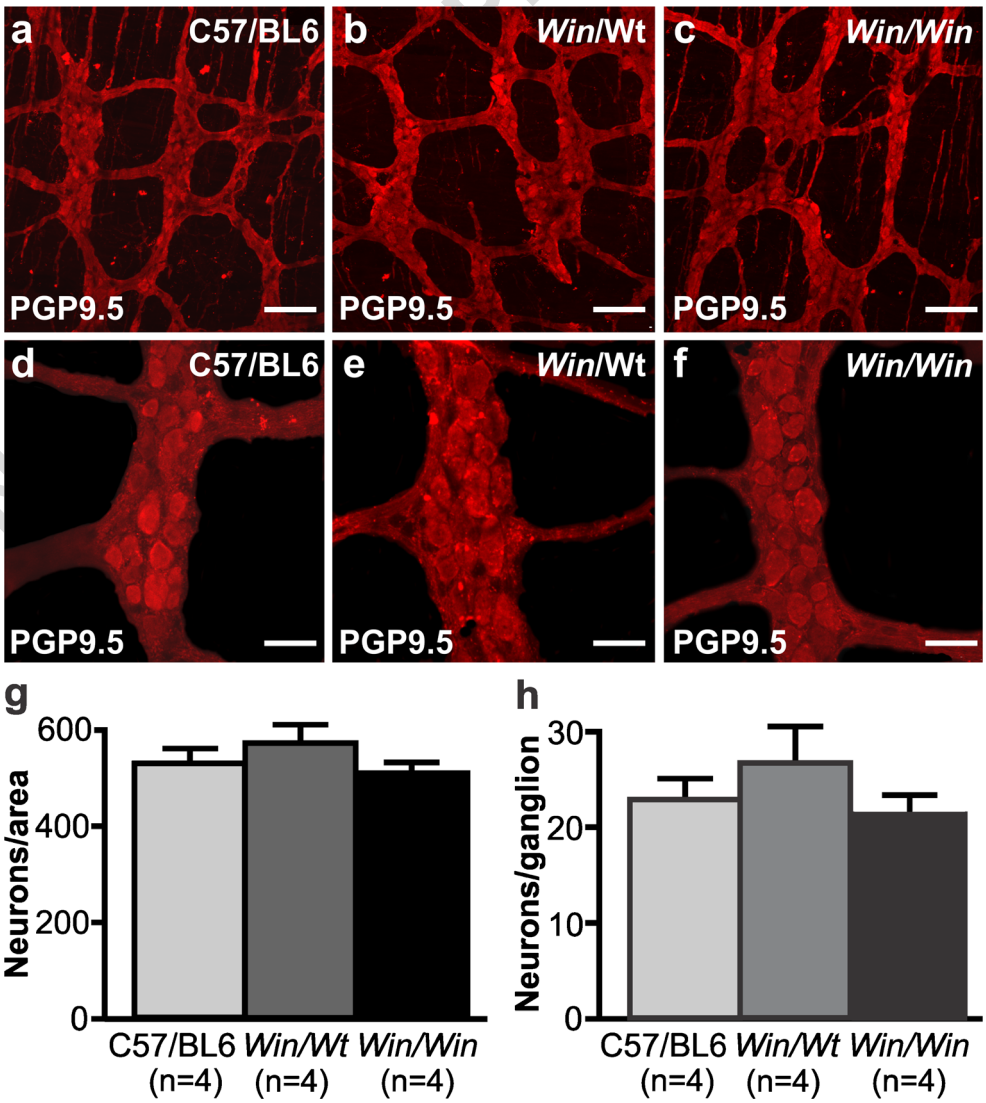

Fig. 5 Total number of myenteric neurons in the distal colon. Myenteric neurons were labeled using antibody against protein gene product (*PGP*) 9.5. Images of PGP9.5-IR neurons within 0.25 mm^2 area (**a**–**c**) and within myenteric ganglia (**d**–**f**). *Scale bars* (**a**–**c**) 100 μm, (**d**–**f**) 50 μm. No significant differences in the average number of myenteric neurons counted per 2 mm^2 area (**g**) or in the average number of myenteric neurons per ganglion (average of 10 ganglia per animal) (**h**) have been observed between all groups. Data are expressed as mean ± SEM. Numbers of animals per group are shown in *parentheses*

compared to C57/BL6 (9.4±0.4 %, $P<0.001$, $n=4$) as well as *Win/Wt* (8.7±0.1 %, $P<0.01$, $n=4$) mice (Fig. 4j–l, n).

No changes in the total number of myenteric neurons and subpopulations of nNOS-IR and cholinergic neurons in the distal colon of Winnie mouse

The total number of neurons in wholemount LMMP preparations of the distal colon was counted using the pan-neuronal marker PGP9.5. The mean number of neurons per surface area (2 mm^2) of the colon was similar in *Win/Win* (548±7, $n=4$), C57/BL6 (559±16, $n=4$) and *Win/Wt* (568±18, $n=4$) mice (Fig. 5a–c, g). No significant differences were observed in the average number of myenteric neurons per ganglion between *Win/Win* (22±2.4, $n=4$), C57/BL6 (23±2.3, $n=4$) and *Win/Wt* (24±3.2, $n=4$) mice (Fig. 5d–f, h).

The number of nNOS-IR neurons in wholemount LMMP preparations of the distal colon was quantified. Immunofluorescence staining showed no significant difference in the average number of nNOS-IR neurons per surface area (2 mm^2) between C57/BL6, *Win/Wt* and *Win/Win* mice (C57/BL6: 390±14; *Win/Wt*: 398±14; *Win/Win*: 389±8; $n=4$/group) (Fig. 6a–c, g) or in the mean number of neurons per ganglion (C57/BL6: 12±1.5; *Win/Wt*: 13±2.2; *Win/Win*: 14±1.3; $n=4$/group) (Fig. 6d–f, h).

The number of cholinergic neurons in wholemount LMMP preparations of the distal colon was counted using anti-ChAT antibody. No significant difference was observed in the mean number of ChAT-IR neurons per surface area (2 mm^2) of the colon between C57/BL6 (535±19, $n=4$), *Win/Wt* (522±21, $n=4$) and *Win/Win* mice (504±19, $n=4$) (Fig. 7a–c, g). Similarly, the average number of ChAT-IR neurons per ganglion was comparable in C57/BL6 (34±2.6, $n=4$), *Win/Wt* (37±3.8, $n=4$) and *Win/Win* mice (34±2.9, $n=4$) (Fig. 7d–f, h).

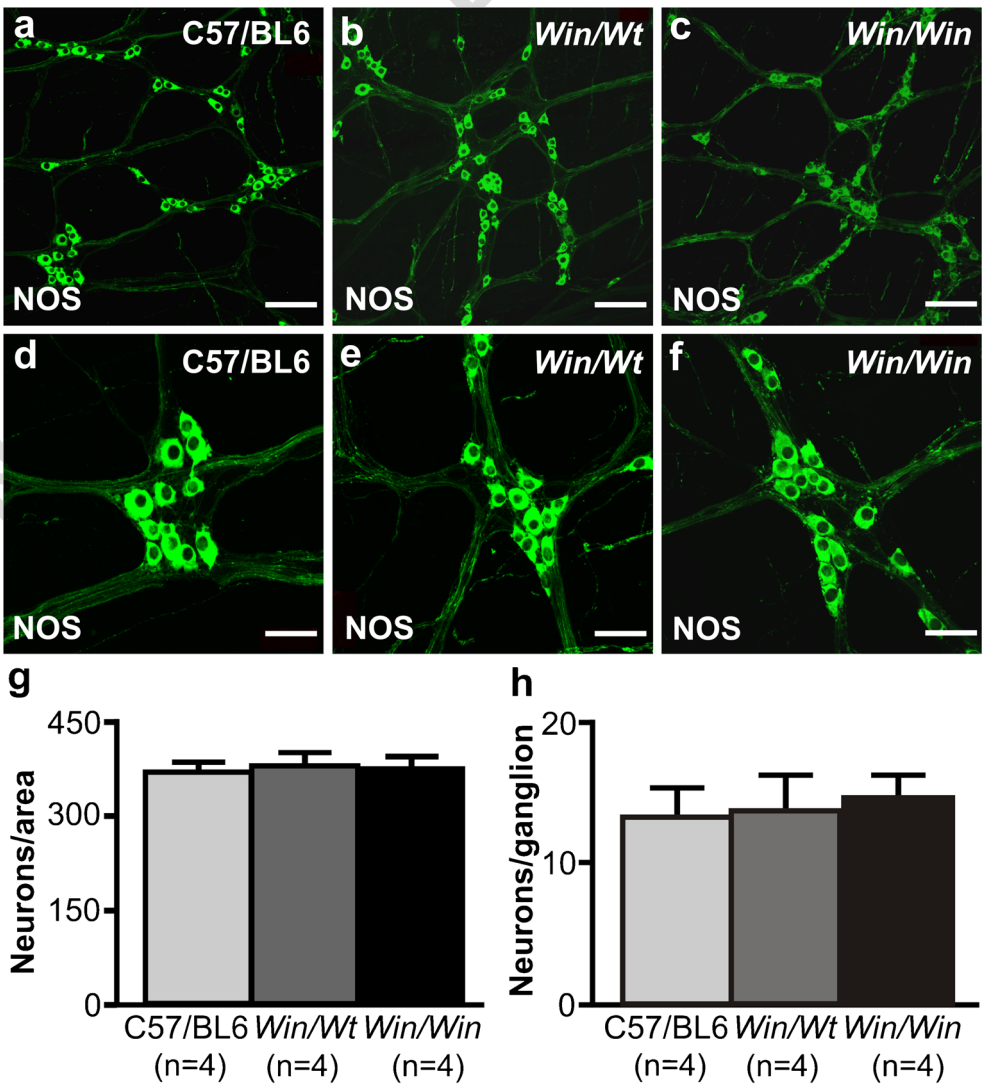

Fig. 6 Number of myenteric nitrergic neurons in the distal colon. Nitric oxide synthase-immunoreactive (NOS-IR) neurons were counted within 2 mm^2 area and within each ganglion in wholemount preparations of the distal colon. Examples of myenteric NOS-IR neurons within 0.25 mm^2 area (**a**–**c**) and within myenteric ganglia (**d**–**f**). *Scale bars* (**a**–**c**) 100 μm, (**d**–**f**) 50 μm. No significant differences in the number of NOS-IR neurons per area (**g**) and per ganglion (**h**) have been found between all groups. Data are expressed as mean ± SEM. Numbers of animals per group are shown in *parentheses*

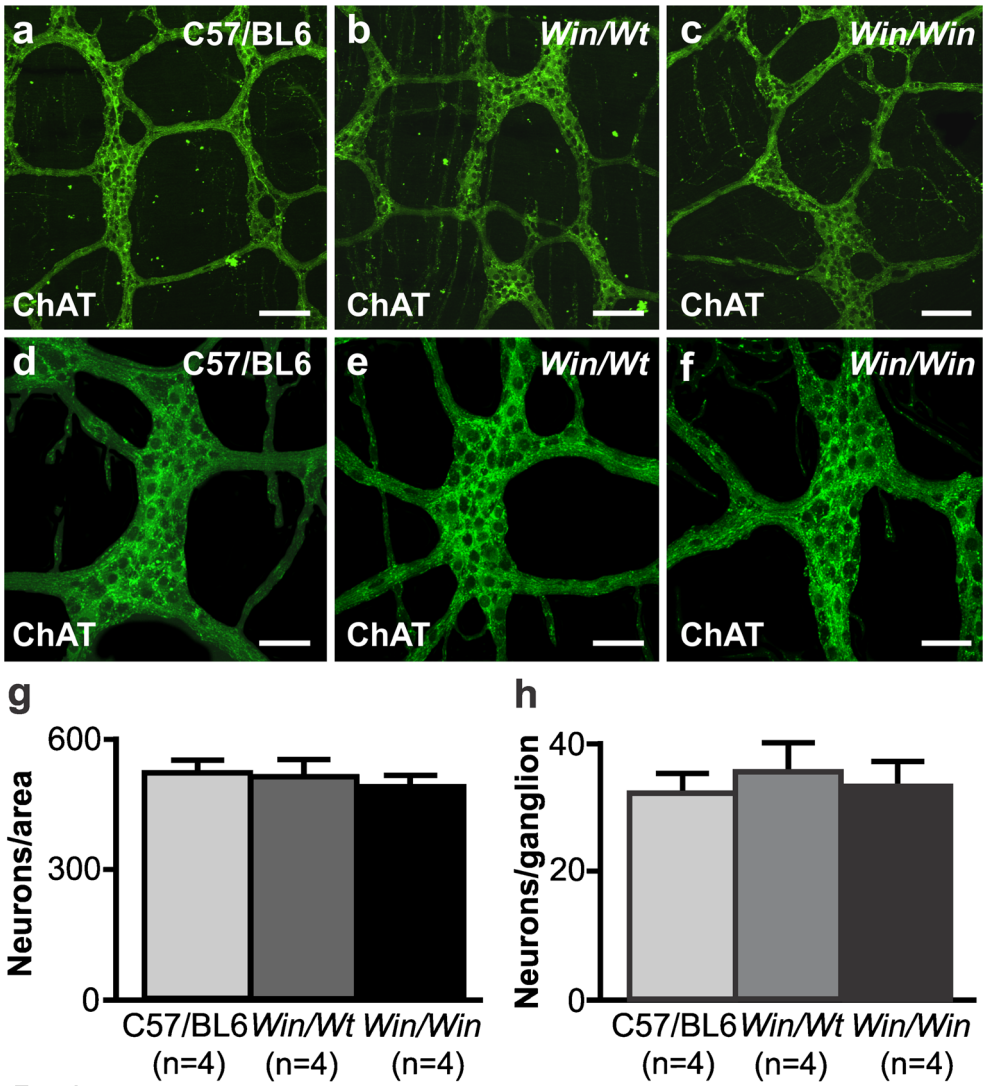

Fig. 7 Number of myenteric cholinergic neurons in the distal colon. Cholinergic neurons labeled with antibody against choline acetyl transferase (ChAT) within 0.25 mm^2 area (**a**–**c**) and within the ganglia (**d**–**f**) in wholemount preparations of the distal colon. *Scale bars* (**a**–**c**) 100 μm, (**d**–**f**) 50 μm. No significant differences in the average number of ChAT-IR neurons per 2 mm^2 area (**g**) and per ganglion (**h**) have been found between all groups. Data are expressed as mean ± SEM. Numbers of animals per group are shown in *parentheses*

Discussion

Animal models of IBD have provided significant contributions to understanding pathophysiological mechanisms as well as development of novel therapeutic strategies for IBD (Mizoguchi and Mizoguchi 2010; Xavier and Podolsky 2007). Although animal models have their limitations and do not reproduce all the pathogenic and clinical features of human IBD, each animal model provided an invaluable tool to study complex physiological and biochemical disease aspects that are difficult to address in humans (Elson et al. 1995; Dothel et al. 2013; Grisham 1993). The *Winnie* mice used in our study develop inflammation in the colon with multiple similarities to human ulcerative colitis, including goblet cell pathology, depleted mucus layer, and distal gradient of colitis as well as a characteristic immune profile (Eri et al. 2011; Heazlewood et al. 2008; Lourenssen et al. 2005; McGuckin et al. 2011). The manifestation of clinical symptoms in *Winnie* mice starts at the age of 6 weeks when animals become young adults. Colitis in *Winnie* mice has a chronic and relapsing nature, a major feature of human IBD. *Winnie* mice carry only a point mutation in *Muc2* gene leading to spontaneous colitis unlike chemically-induced models and some other chronic models which require pathogens to develop colitis (e.g., IL-$10^{-/-}$ mice) (Uhlig and Powrie 2009; Wirtz and Neurath 2007). In this study, we used 12- to 16-week-old *Winnie* mice all of which had active colitis with symptoms of perianal bleeding and diarrhea confirmed by increased fecal water content and lack of weight gain. By this age, chronic inflammation induced morphological changes in the colon including increase in its length and marked thickening of the intestinal wall which may contribute to colonic dysmotility present in these mice (unpublished data). Together with the mucosal damage and leukocyte infiltration observed in all *Winnie* mice in this study, these are the hallmark features of chronic intestinal inflammation. Muscular hypertrophy, changes in colon length and similar

JnlID 441_ArtID 2251_Proof# 1 - 09/07/2015

gross morphological changes have been described previously in other models of chronic intestinal inflammation (Grisham 1993; Elson et al. 1995; Rivera-Nieves et al. 2003).

Inflammation in *Winnie* mice was associated with significant structural damage to the colonic innervation which was investigated for the first time in this study. The results of this study have demonstrated decrease in the density of cholinergic, noradrenergic and sensory nerve fibers projecting to the myenteric plexus, and unchanged total number of neurons and numbers of nitrergic and cholinergic neurons in the myenteric plexus of the distal colon from *Winnie* mice.

Significant reduction of the density of VAChT-IR cholinergic nerve fibers observed in the colon tissues from *Winnie* mice in our study is consistent with previous work conducted in the colon tissues from ulcerative colitis patients (Jönsson et al. 2007). It has been established that acetylcholine attenuates the release of pro-inflammatory cytokines (Borovikova et al. 2000; Ulloa 2005) and thereby could control systemic inflammation and modulate immune response. Other studies further demonstrated that cholinergic pathways also modulated experimental colitis in rats by using acetylcholinesterase inhibitors (Miceli and Jacobson 2003) or vagotomy (Ghia et al. 2006). Previous studies showed impaired release of acetylcholine from the inflamed rat intestine (Collins et al. 1989). Alterations in functions of cholinergic fibers in *Winnie* mice should be further investigated.

Noradrenergic neurons of the sympathetic celiac and the superior mesenteric ganglia innervate the smooth muscles and enteric ganglia in the colon and modulate motility, secretion, blood flow, and immune system activation (Cervi et al. 2014; Lomax et al. 2010; Miolan and Niel 1996; Straub et al. 2008; Vasina et al. 2008). Results of our study demonstrated that the density of noradrenergic nerve fibers identified by TH immunoreactivity was significantly reduced in the colon tissues from *Winnie* mice. This is consistent with the results of previous studies in patients with Crohn's disease (Belai et al. 1997; Straub et al. 2008), and in mouse models of DSS and TNBS-induced colitis (Lomax et al. 2007b; Straub et al. 2005). A large body of evidence obtained from animal models of gastrointestinal inflammation indicated marked changes in sympathetic neuronal excitability (Dong et al. 2008), neurotransmitter release (Blandizzi et al. 2003; Swain et al. 1991) and structure of noradrenergic nerve fibers (Dvorak et al. 1980; Dvorak and Silen 1985; Magro et al. 2002; Straub et al. 2008). Decreased colonic mucosal norepinephrine concentration was observed in Crohn's disease patients (Magro et al. 2002). In addition, colitis impairs noradrenergic regulation of submucosal arterioles and mesenteric arteries (Birch et al. 2008; Lomax et al. 2007b).

Similar to previous studies (Lourenssen et al. 2005; Straub et al. 2005), no TH-IR cell bodies were found in the myenteric plexus of *Winnie* or C57/BL6 mice. However, TH-IR neurons were previously reported to be present in the mouse and human gut. TH immunoreactivity was observed in a very small proportion (less than 0.5 %) of myenteric neurons in the ileum of adult Balb/c mice (Qu et al. 2008). TH-IR neurons constituted about 9 % of myenteric and 13 % of submucosal neurons in the ileum of adult CD-1 mice (Li et al. 2004). TH-IR myenteric and submucosal neurons were found in humans throughout the gastrointestinal tract, but most frequently in the esophagus (Wakabayashi et al. 1989). In our study, cell bodies of TH-IR neurons were not found in the distal colon of C57/BL6 or *Winnie* mice. Whether this discrepancy is due to the differences between species and mouse strains or regional differences needs to be further investigated. However, the presence of TH-IR fibers from intrinsic TH-positive neurons should not be excluded as we have not investigated the entire length of the intestine.

Anti-CGRP antibody was used to label sensory fibers including extrinsic spinal and vagal primary sensory afferent as well as intrinsic sensory fibers containing and releasing CGRP (Grider 2003; Kressel et al. 1994; Qu et al. 2008). CGRP was found to be reduced in the inflamed bowel in animal models of chemically-induced colitis (Eysselein et al. 1991; Miampamba et al. 1992; Miampamba and Sharkey 1998). Moreover, tissues from patients with Crohn's disease and ulcerative colitis also showed decrease in the number and density of CGRP-positive nerve fibers in the colonic mucosa (Koch et al. 1987; Eysselein et al. 1992).

Our data demonstrated that, although significant reduction in all types of fibers analyzed in this study was observed, CGRP-IR fibers were the most affected compared to other types of fibers in *Winnie* mice with the loss of about 65 % of CGRP-IR fibers in cross-sections. CGRP-IR sensory fibers extensively supply the mucosa and submucosa where chronic inflammation is the most prominent in *Winnie* mice. CGRP released from sensory nerve fibers plays important anti-inflammatory and protective roles: it facilitates mucus production and controls blood flow in the gastrointestinal mucosa (Holzer 2007). It has been suggested that during inflammation there is a sustained increased release of CGRP, leading to depletion of CGRP fibers (Eysselein et al. 1992). Loss of CGRP-IR sensory fibers and sensory neuron dysfunction impair mucosal protection (Holzer 2007). The loss of about 52 % of TH-IR noradrenergic fibres within myenteric ganglia observed in our study might contribute to impairment of motility, secretion, blood flow and gastrointestinal immunity in *Winnie* mice which needs to be further investigated. It was suggested that the loss of

noradrenergic fibers is a pro-inflammatory signal in the chronic phase of the intestinal inflammation (Straub et al. 2008). On the other hand, the density of VAChT-IR cholinergic fibers was less reduced in cross-sections (by 27 %) of the colon from *Winnie* mice. This might be due to the extensive projection of cholinergic fibers to the muscle layer where immune infiltration is less prominent. Nevertheless, significant reduction of VAChT-IR fibers within the myenteric ganglia (by 40 %) suggests that excitatory cholinergic neurotransmission is reduced, leading to impaired motility and symptoms of diarrhea observed in *Winnie* mice. Given the potent anti-inflammatory effect of the cholinergic innervation (Matteoli and Boeckxstaens 2013), the loss of VAChT fibers may have an important impact on immune homeostasis in *Winnie* mice.

Whether the loss of nerve fibers in *Winnie* mice is a result of chronic inflammation or if *Winnie* mice are born with altered intestinal innervation which contributes to initial pathological changes in the mucosa leading to inflammation needs to be further elucidated.

Our findings showed that the number of myenteric neurons remained unchanged in the *Winnie* mouse distal colon. There is a great degree of controversy in the literature regarding the number of myenteric neurons in the inflamed intestine. Some studies reported increase, while others reported decrease or no change in the number of myenteric neurons in tissues from animal models of intestinal inflammation and from IBD patients (Table 2). Decreased number of neurons in the myenteric plexus in both wholemount preparations and cross-sections was reported in most animal models of chemically-induced intestinal inflammation, except a study reporting no changes in wholemount preparations and cross-sections of the colon from rats with DSS-induced colitis (Winston et al. 2013). In human tissues, most of the studies were performed in transverse or cross-sections showing either increase, decrease or no change in the number of myenteric neurons (Table 2). A study performed in wholemount preparations of the colon from patients with ulcerative colitis demonstrated no changes in the number of myenteric neurons (Neunlist et al. 2003). This is consistent with the results of our study in wholemount preparations of the distal colon from *Winnie* mice with chronic inflammation. Our results demonstrated that the number of cholinergic (ChAT-IR excitatory muscle motor and interneurons) and nitrergic (NOS-IR inhibitory muscle motor and interneurons) neurons in the myenteric plexus were unaltered in the distal colon of *Winnie* mice. These results are consistent with findings in rats with DSS-induced colitis (Winston et al. 2013) and in patients with ulcerative colitis (Neunlist et al. 2003). Further studies need to investigate the gene expression of proteins regulating the synthesis of ACh and NO which can be altered, even though the number of neurons is not changed, leading to intestinal dysmotility (Winston et al. 2013). However, reductions in the density of nerve fibers observed in *Winnie* mice might lead to decreased neuropeptide release and changes in the neurotransmission affecting gastrointestinal functions. Functional studies investigating these changes in *Winnie* mice are warranted in the future.

In conclusion, the present study demonstrates that colitis in *Winnie* mice is associated with significant impairment of distal colon innervation. Changes in the cholinergic, noradrenergic and sensory innervation observed in *Winnie* mice were similar to those observed in ulcerative colitis patients.

t2.1 **Table 2** Effect of intestinal inflammation on the number of neurons in the myenteric plexus

t2.2	Species	Pathology/model	Tissues studied	Preparations	Number of neurons	References
t2.3	Human	Ulcerative colitis	Colon	Transverse sections	Threefold increase	(Storsteen et al. 1953)
t2.4	Human	Crohn's disease	Ileum	Transverse sections	Threefold increase	(Davis et al. 1955)
t2.5	Human	Ulcerative colitis	Colon	Cross-sections	61 % decrease	(Bernardini et al. 2012)
t2.6	Human	Ulcerative colitis	Colon	Wholemounts	No change	(Neunlist et al. 2003)
t2.7	Human	Ulcerative colitis	Colon	Transverse sections	No change	(Villanacci et al. 2008)
t2.8	Guinea-pig	TNBS	Colon	Wholemounts	15 % decrease	(Linden et al. 2005)
t2.9	Guinea-pig	TNBS	Ileum	Wholemounts	17 % decrease	(Nurgali et al. 2011)
t2.10	Mouse	DNBS	Colon	Wholemounts	50 % decrease	(Boyer et al. 2005)
t2.11	Rat	DNBS	Colon	Cross-sections	50 % decrease	(Sanovic et al. 1999)
t2.12	Rat	TNBS	Colon	Cross-sections	Decrease or absent (qualitative analysis)	(Poli et al. 2001)
t2.13	Rat	TNBS	Colon	Wholemounts	33 % decrease	(Lin et al. 2005)
t2.14	Rat	TNBS	Colon	Wholemounts	20 % decrease	(Sarnelli et al. 2009)
t2.15	Rat	DSS	Colon	Wholemounts	No change	(Winston et al. 2013)

Q3

Acknowledgments This study was supported by the Australian National Health & Medical Research Council project grant 1032414 and a Victoria University research support grant.

Conflict of interest The authors of this manuscript do not have any potential conflicts to disclose.

Role of authors AAR performed experiments, analyzed data and wrote the manuscript. AMR performed experiments, analyzed data and contributed to manuscript writing. VJ contributed to processing tissues for immunohistochemical and histological studies. RE and KN developed the concept and edited manuscript. KN obtained funding and supervised the study.

Funding This study is supported by the Australian National Health & Medical Research Council project grant 1032414 and a Victoria University Research Development Grant.

References

Belai A, Boulos PB, Robson T, Burnstock G (1997) Neurochemical coding in the small intestine of patients with Crohn's disease. Gut 40: 767–774

Bernardini N, Segnani C, Ippolito C, De Giorgio R, Colucci R, Faussone-Pellegrini MS, Chiarugi M, Campani D, Castagna M, Mattii L, Blandizzi C, Dolfi A (2012) Immunohistochemical analysis of myenteric ganglia and interstitial cells of Cajal in ulcerative colitis. J Cell Mol Med 16:318–327

Birch D, Knight GE, Boulos PB, Burnstock G (2008) Analysis of innervation of human mesenteric vessels in non-inflamed and inflamed bowel – a confocal and functional study. Neurogastroenterol Motil 20:660–670

Blandizzi C, Fornai M, Colucci R, Baschiera F, Barbara G, Giorgio RD, Ponti FD, Breschi MC, Tacca MD (2003) Altered prejunctional modulation of intestinal cholinergic and noradrenergic pathways by α2-adrenoceptors in the presence of experimental colitis. Br J Pharmacol 139:309–320

Borovikova LV, Ivanova S, Zhang M, Yang H, Botchkina GI, Watkins LR, Wang H, Abumrad N, Eaton JW, Tracey KJ (2000) Vagus nerve stimulation attenuates the systemic inflammatory response to endotoxin. Nature 405:458–462

Boyer L, Ghoreishi M, Templeman V, Vallance BA, Buchan AM, Jevon G, Jacobson K (2005) Myenteric plexus injury and apoptosis in experimental colitis. Auton Neurosci 117:41–53

Buisine MP, Desreumaux P, Leteurtre E, Copin MC, Colombel JF, Porchet N, Aubert JP (2001) Mucin gene expression in intestinal epithelial cells in Crohn's disease. Gut 49:544–551

Cervi AL, Lukewich MK, Lomax AE (2014) Neural regulation of gastrointestinal inflammation: role of the sympathetic nervous system. Auton Neurosci 182:83–88

Chen BN, Sharrad DF, Hibberd TJ, Zagorodnyuk VP, Costa M, Brookes SJ (2015) Neurochemical characterization of extrinsic nerves in myenteric ganglia of the guinea pig distal colon. J Comp Neurol 523(5):742–56

Collins SM, Blennerhassett PA, Blennerhassett MG, Vermillion DL (1989) Impaired acetylcholine release from the myenteric plexus of *Trichinella*-infected rats. Am J Physiol 257:G898–G903

Davis D, Dockerty MB, Mayo CM(1955) The myenteric plexus in regional enteritis: a study of the number of ganglion cells in the ileum in 24 cases. Surg Gynecol Obstet 101:208–216

Dong XX, Thacker M, Pontell L, Furness JB, Nurgali K (2008) Effects of intestinal inflammation on specific subgroups of guinea-pig celiac ganglion neurons. Neurosci Lett 444:231–235

Dothel G, Vasina V, Barbara G, De Ponti F (2013) Animal models of chemically induced intestinal inflammation: predictivity and ethical issues. Pharmacol Ther 139:71–86

Dvorak AM, Silen W (1985) Differentiation between Crohn's disease and other inflammatory conditions by electron microscopy. Ann Surg 201:53–63

Dvorak AM, Osage JE, Monahan RA, Dickersin GR (1980) Crohn's disease: transmission electron microscopic studies. III. Target tissues, proliferation of and injury to smooth muscle and the autonomic nervous system. Hum Pathol 11:620–634

Elson CO, Sartor RB, Tennyson GS, Riddell RH (1995) Experimental models of inflammatory bowel disease. Gastroenterology 109: 1344–1367

Eri RD, Adams RJ, Tran TV, Tong H, Das I, Roche DK, Oancea I, Png CW, Jeffery PL, Radford-Smith GL, Cook MC, Florin TH, McGuckin MA (2011) An intestinal epithelial defect conferring ER stress results in inflammation involving both innate and adaptive immunity. Mucosal Immunol 4:354–364

Eysselein VE, Reinshagen M, Cominelli F, Sternini C, Davis W, Patel A, Nast CC, Bernstein D, Anderson K, Khan H et al (1991) Calcitonin gene-related peptide and substance P decrease in the rabbit colon during colitis. A time study. Gastroenterology 101:1211–1219

Eysselein VE, Reinshagen M, Patel A, Davis W, Nast C, Sternini C (1992) Calcitonin gene-related peptide in inflammatory bowel disease and experimentally induced colitis. Ann N Y Acad Sci 657: 319–27

Furness JB (2012) The enteric nervous system and neurogastroenterology. Nat Rev Gastroenterol Hepatol 9:286–294

Geboes K, Collins S (1998) Structural abnormalities of the nervous system in Crohn's disease and ulcerative colitis. Neurogastroenterol Motil 10:189–202

Ghia JE, Blennerhassett P, Kumar-Ondiveeran H, Verdu EF, Collins SM (2006) The vagus nerve: a tonic inhibitory influence associated with inflammatory bowel disease in a murine model. Gastroenterology 131:1122–1130

Grider JR (2003) Neurotransmitters mediating the intestinal peristaltic reflex in the mouse. J Pharmacol Exp Ther 307:460–467

Grisham MB (1993) Animal models of inflammatory bowel disease. Curr Opin Gastroenterol 9:524–533

Heazlewood CK, Cook MC, Eri R, Price GR, Tauro SB, Taupin D, Thornton DJ, Chin WP, Crockford TL, Cornall RJ, Adams R, Kato M, Nelms KA, Hong NA, Florin THJ, Goodnow CC, McGuckin MA (2008) Aberrant mucin assembly in mice causes endoplasmic reticulum stress and spontaneous inflammation resembling ulcerative colitis. PLoS Med 5:0440–0460

Holzer P (2007) Role of visceral afferent neurons in mucosal inflammation and defence. Curr Opin Pharmacol 7(6):563–569

Jönsson M, Norrgård Ö, Forsgren S (2007) Presence of a marked nonneuronal cholinergic system in human colon: study of normal colon and colon in ulcerative colitis. Inflamm Bowel Dis 13:1347–1356

Kajimoto Y, Hashimoto T, Shirai Y, Nishino N, Kuno T, Tanaka C (1992) cDNA cloning and tissue distribution of a ratubiquitin carboxyl-terminal hydrolase PGP9.5.J Biochem112:28–32

Kaser A, Zeissig S, Blumberg RS (2010) Inflammatory bowel disease. Annu Rev Immunol 28(28):573–621

Koch TR, Carney JA, Go VL (1987) Distribution and quantitation of gut neuropeptides in normal intestine and inflammatory bowel diseases. Dig Dis Sci 32:369–376

Krauter EM, Strong DS, Brooks EM, Linden DR, Sharkey KA, Mawe GM (2007) Changes in colonic motility and the electrophysiological properties of myenteric neurons persist following recovery from trinitrobenzene sulfonic acid colitis in the guinea pig. Neurogastroenterol Motil 19:990–1000

Kressel M, Berthoud HR, Neuhuber WL (1994) Vagal innervation of the rat pylorus: an anterograde tracing study using carbocyanine dyes

and laser scanning confocal microscopy. Cell Tissue Res 275:109–123

Li ZS, Pham TD, Tamir H, Chen JJ, Gershon MD (2004) Enteric dopaminergic neurons: definition, developmental lineage, and effects of extrinsic denervation. J Neurosci 24(6):1330–9

Lin A, Lourenssen S, Stanzel RD, Blennerhassett MG (2005) Nervegrowth factor sensitivity is broadly distributed among myenteric neurons ofthe rat colon. J Comp Neurol 490:194–206

Linden DR, Sharkey KA, Mawe GM (2003) Enhanced excitability of myenteric AH neurones in the inflamed guinea-pig distal colon. J Physiol 547:589–601

Linden DR, Couvrette JM, Ciolino A, McQuoid C, Blaszyk H, Sharkey KA, Mawe GM (2005) Indiscriminate loss of myenteric neurones in the TNBS-inflamed guinea-pig distal colon. Neurogastroenterol Motil 17:751–760

Lindgren S, Lilja B, Rosen I, Sundkvist G (1991) Disturbed autonomic nerve function in patients with Crohn's disease. Scand J Gastroenterol 26:361–366

Lindgren S, Stewenius J, Sjolund K, Lilja B, Sundkvist G (1993) Autonomic vagal nerve dysfunction in patients with ulcerative colitis. Scand J Gastroenterol 28:638–642

Lomax AE, Fernández E, Sharkey KA (2005) Plasticity of the enteric nervous system during intestinal inflammation. Neurogastroenterol Motil 17:4–15

Lomax AE, O'Hara JR, Hyland NP, Mawe GM, Sharkey KA (2007a) Persistent alterations to enteric neural signaling in the guinea pig colon following the resolution of colitis. Am J Physiol 292:G482–G491

Lomax AE, O'Reilly M, Neshat S, Vanner SJ (2007b) Sympathetic vasoconstrictor regulation of mouse colonic submucosal arterioles is altered in experimental colitis. J Physiol 583:719–730

Lomax AE, Sharkey KA, Furness JB (2010) The participation of the sympathetic innervation of the gastrointestinal tract in disease states. Neurogastroenterol Motil 22:7–18

Lourenssen S, Wells RW, Blennerhassett MG (2005) Differential responses of intrinsic and extrinsic innervation of smooth muscle cells in rat colitis. Exp Neurol 195:497–507

Magro F, Vieira-Coelho MA, Fraga S, Serrão MP, Veloso FT, Ribeiro T, Soares-da-Silva P (2002) Impaired synthesis or cellular storage of norepinephrine, dopamine, and 5-hydroxytryptamine in human inflammatory bowel disease. Dig Dis Sci 47:216–224

Matteoli G, Boeckxstaens GE (2013) The vagal innervation of the gut and immune homeostasis. Gut 62:1214–1222

Mawe GM, Strong DS, Sharkey KA (2009) Plasticity of enteric nerve functions in the inflamed and postinflamed gut. Neurogastroenterol Motil 21:481–491

Mayer EA, Gebhart GF (1994) Basic and clinical aspects of visceral hyperalgesia. Gastroenterology 107:271–293

McGuckin MA, Eri RD, Das I, Lourie R, Florin TH (2011) Intestinal secretory cell ER stress and inflammation. Biochem Soc Trans 39: 1081–1085

Miampamba M, Sharkey KA (1998) Distribution of calcitonin gene-related peptide, somatostatin, substance P and vasoactive intestinal polypeptide in experimental colitis in rats. Neurogastroenterol Motil 10:315–329

Miampamba M, Chery-Croze S, Chayvialle JA (1992) Spinal and intestinal levels of substance P, calcitonin gene-related peptide and vasoactive intestinal polypeptide following perendoscopic injection of formalin in rat colonic wall. Neuropeptides 22:73–80

Miceli PC, Jacobson K (2003) Cholinergic pathways modulate experimental dinitrobenzene sulfonic acid colitis in rats. Auton Neurosci 105:16–24

Miolan JP, Niel JP (1996) The mammalian sympathetic prevertebral ganglia: integrative properties and role in the nervous control of digestive tract motility. J Auton Nerv Syst 58:125–138

Mizoguchi A (2012) Animal models of inflammatory bowel disease. Prog Mol Biol Transl Sci 105:263–320

Mizoguchi A, Mizoguchi E (2010) Animal models of IBD: linkage to human disease. Curr Opin Pharmacol 10:578–587

Moynes DM, Lucas GH, Beyak MJ, Lomax AE (2014) Effects of inflammation on the innervation of the colon. Toxicol Pathol 42:111–117

Nagatsu T (1989) The human tyrosine hydroxylase gene. Cell Mol Neurobiol 9:313–321

Neunlist M, Aubert P, Toquet C, Oreshkova T, Barouk J, Lehur PA, Schemann M, Galmiche JP (2003) Changes in chemical coding of myenteric neurones in ulcerative colitis. Gut 52:84–90

Nurgali K, Nguyen TV, Matsuyama H, Thacker M, Robbins HL, Furness JB (2007) Phenotypic changes of morphologically identified guinea-pig myenteric neurons following intestinal inflammation. J Physiol 583:593–609

Nurgali K, Nguyen TV, Thacker M, Pontell L, Furness JB (2009) Slow synaptic transmission in myenteric AH neurons from the inflamed guinea pig ileum. Am J Physiol 297:G582–G593

Nurgali K, Qu Z, Hunne B, Thacker M, Pontell L, Furness JB (2011) Morphological and functional changes in guinea-pig neurons projecting to the ileal mucosa at early stages after inflammatory damage. J Physiol 589:325–339

Podolsky DK (2002) Inflammatory bowel disease. N Engl J Med 347: 417–429

Poli E, Lazzaretti M, Grandi D, Pozzoli C, Coruzzi G (2001) Morphological and functional alterations of the myenteric plexus in rats with TNBS-induced colitis. Neurochem Res 26:1085–1093

Qu ZD, Thacker M, Castelucci P, Bagyánszki M, Epstein ML, Furness JB (2008) Immunohistochemical analysis of neuron types in the mouse small intestine. Cell Tissue Res 334:147–161

Rao SSC, Read NW (1990) Gastrointestinal motility in patients with ulcerative colitis. Scand J Gastroenterol 25:22–28

Rivera-Nieves J, Bamias G, Vidrich A, Marini M, Pizarro TT, McDuffie MJ, Moskaluk CA, Cohn SM, Cominelli F (2003) Emergence of perianal fistulizing disease in the SAMP1/YitFc mouse, a spontaneous model of chronic ileitis. Gastroenterology 124:972–982

Robinson AM, Sakkal S, Park A, Jovanovska V, Payne NL, Carbone SE, Miller S, Bornstein JC, Bernard C, Boyd R, Nurgali K (2014) Mesenchymal stem cells and conditioned medium avert enteric neuropathy and colon dysfunction in guinea-pig TNBS-induced colitis. Am J Physiol 307:G1115–29

Sanovic S, Lamb DP, Blennerhassett MG (1999) Damage to the enteric nervous system in experimental colitis. Am J Pathol 155:1051–1057

Sarnelli G, De Giorgio R, Gentile F, Calì G, Grandone I, Rocco A, Cosenza V, Cuomo R, D'Argenio G (2009) Myenteric neuronal loss in rats with experimental colitis: role of tissue transglutaminase-induced apoptosis. Digest Liver Diseases 41:185–193

Storsteen KA, Kernohan JW, Bargen JA(1953) The myenteric plexus in the presence of chronic ulcerative colitis. Surg Gynecol Obstet 97: 335–343

Straub RH, Stebner K, Härle P, Kees F, Falk W, Schölmerich J (2005) Key role of the sympathetic microenvironment for the interplay of tumour necrosis factor and interleukin 6 in normal but not in inflamed mouse colon mucosa. Gut 54:1098–1106

Straub RH, Grum F, Strauch U, Capellino S, Bataille F, Bleich A, Falk W, Schölmerich J, Obermeier F (2008) Anti-inflammatory role of sympathetic nerves in chronic intestinal inflammation. Gut 57:911–921

Strober W, Fuss I, Mannon P (2007) The fundamental basis of inflammatory bowel disease. J Clin Invest 117:514–521

Swain MG, Blennerhassett PA, Collins SM (1991) Impaired sympathetic nerve function in the inflamed rat intestine. Gastroenterology 100: 675–682

Uhlig HH, Powrie F (2009) Mouse models of intestinal inflammation as tools to understand the pathogenesis of inflammatory bowel disease. Eur J Immunol 39:2021–2026

JnlID 441_ArtID 2251_Proof# 1 - 09/07/2015

Ulloa L (2005) The vagus nerve and the nicotinic anti-inflammatory pathway. Nat Rev Drug Discov 4:673–684

Villanacci V, Bassotti G, Nascimbeni R, Antonelli E, Cadei M, Fisogni S, Salerni B, Geboes K (2008) Enteric nervous system abnormalities in inflammatory bowel diseases. Neurogastroenterol Motil 20:1009–1016

Van Klinken BJW, Van Der Wal JWG, Einerhand A, Büller HA, Dekker J (1999) Sulphation and secretion of the predominant secretory human colonic mucin MUC2 in ulcerative colitis. Gut 44:387–393

Vasina V, Abu-gharbieh E, Barbara G, De Giorgio R, Colucci R, Blandizzi C, Bernardini N, Croci T, Del Tacca M, De Ponti F (2008) The β3-adrenoceptor agonist SR58611A ameliorates experimental colitis in rats. Neurogastroenterol Motil 20:1030–1041

Wafai L, Taher M, Jovanovska V, Bornstein JC, Dass CR, Nurgali K (2013) Effects of oxaliplatin on mouse myenteric neurons and colonic motility. Front Neurosci 7:1–8

Wakabayashi K, Takahashi H, Ohama E, Ikuta F (1989) Tyrosine hydroxylase-immunoreactive intrinsic neurons in the Auerbach's and Meissner's plexuses of humans. Neurosci Lett 96(3):259–63

Weihe E, Tao-Cheng JH, Schäfer MKH, Erickson JD, Eiden LE (1996) Visualization of the vesicular acetylcholine transporter in cholinergic nerve terminals and its targeting to a specific population of small synaptic vesicles. Proc Natl Acad Sci U S A 93:3547–3552

Winston JH, Li Q, Sarna SK (2013) Paradoxical regulation of ChAT and nNOS expression in animal models of Crohn's colitis and ulcerative colitis. Am J Physiol 305:G295–G302

Wirtz S, Neurath MF (2007) Mouse models of inflammatory bowel disease. Adv Drug Deliv Rev 59:1073–1083

Xavier RJ, Podolsky DK (2007) Unravelling the pathogenesis of inflammatory bowel disease. Nature 448(7152):427–34

AUTHOR QUERIES

AUTHOR PLEASE ANSWER ALL QUERIES.

Q1. Please check if the affiliations are presented correctly.
Q2. Miampamba et al. 1998 has been changed to Miampamba and Sharkey 1998 as per the reference list. Please check if okay.
Q3. Note that all seven missing reference details queried in this table have been added to the Reference List by the Copyeditor. Author to check and confirm.